

3D (bio)printing of magnetic hydrogels: Formulation and applications in tissue engineering

*Original*

3D (bio)printing of magnetic hydrogels: Formulation and applications in tissue engineering / Almeida, D., Sanjuan-Alberte, P., Silva, J.C., Ferreira, F.C.. - In: INTERNATIONAL JOURNAL OF BIOPRINTING. - ISSN 2424-8002. - 10:1(2024), pp. 1-19. [10.36922/ijb.0965]

*Availability:*

This version is available at: 11583/2997660 since: 2025-02-20T21:02:48Z

*Publisher:*

AccScience Publishing

*Published*

DOI:10.36922/ijb.0965

*Terms of use:*

This article is made available under terms and conditions as specified in the corresponding bibliographic description in the repository

*Publisher copyright*

(Article begins on next page)

## REVIEW ARTICLE

3D (bio)printing of magnetic hydrogels:  
Formulation and applications in tissue  
engineering**Duarte Almeida<sup>1</sup>, Paola Sanjuan-Alberte<sup>1,2\*</sup>, João C. Silva<sup>1,2\*</sup>, and  
Frederico Castelo Ferreira<sup>1,2</sup>**<sup>1</sup>Department of Bioengineering and Institute for Bioengineering and Biosciences, Instituto Superior Técnico, Universidade de Lisboa, Av. Rovisco Pais, 1049-001 Lisbon, Portugal<sup>2</sup>Associate Laboratory i4HB—Institute for Health and Bioeconomy, Instituto Superior Técnico, Universidade de Lisboa, Av. Rovisco Pais, 1049-001 Lisbon, Portugal

(This article belongs to the *Special Issue: Bioprinting-based strategies for regenerative medicine, drug development and food technology applications*)

**Abstract**

Hydrogels have been widely explored in tissue engineering due to their versatile and customizable properties in terms of their mechanical, biological, and chemical features. These properties allow them to recreate the physiological structures of the extracellular matrix in a highly hydrated state. Particularly, magnetic hydrogels have shown great promise due to their biocompatibility, mechanical attributes, and possibility to be controlled remotely. Three-dimensional (3D) (bio)printing has emerged as an efficient method to fabricate 3D complex scaffolds from hydrogels with a defined structure and porous microarchitecture, which is crucial for cell proliferation, migration, and differentiation. Therefore, combining magnetic-responsive biomaterials with bioprinting strategies offers numerous advantages for tissue engineering applications. Despite the large number of reviews on magnetic hydrogels available in the literature, they lack a clear focus on the fabrication of hydrogels through a 3D (bio)printing process. Thus, this review highlights not only the main characteristics and fabrication methods of magnetic nanoparticles (MNPs), but also the strategies for their incorporation into hydrogels. Furthermore, we also provide an overview of the current state of the art in injectable magnetic hydrogels, which have the potential to be used as bioinks for 3D (bio)printing, envisaging several applications in the regenerative medicine and biomedical engineering fields.

**\*Corresponding authors:**

João C. Silva

(joao.f.da.silva@tecnico.ulisboa.pt)

Paola Sanjuan-Alberte

(paola.alberte@tecnico.ulisboa.pt)

**Citation:** Almeida D, Sanjuan-Alberte P, Silva JC, Ferreira FC. 3D (bio)printing of magnetic hydrogels: Formulation and applications in tissue engineering. *Int J Bioprint.* 2024;10(1): 0965.  
doi: 10.36922/ijb.0965

**Received:** May 20, 2023**Accepted:** June 20, 2023**Published Online:** August 23, 2023**Copyright:** © 2023 Author(s).

This is an Open Access article distributed under the terms of the Creative Commons Attribution License, permitting distribution, and reproduction in any medium, provided the original work is properly cited.

**Publisher's Note:** AccScience Publishing remains neutral with regard to jurisdictional claims in published maps and institutional affiliations.

**Keywords:** Magnetic hydrogels; Magnetic stimulation, Tissue engineering; 3D (bio)printing; Magnetic nanoparticles

**1. Introduction**

Hydrogels are three-dimensional (3D) polymeric structures, of natural or synthetic origin,<sup>1</sup> able to incorporate large amounts of water into their structure. These materials are formed through physical and/or chemical crosslinking processes and present highly versatile physical, chemical, mechanical, rheological, and biological characteristics.<sup>2</sup> Typically, hydrogels are mechanically soft, rendering them useful for soft tissue engineering applications, and possess an interconnected porous network that is highly

favorable for cell adhesion and proliferation. Several types of hydrogels have been studied for biomedical applications based on the desired functional outcome, with applications in cartilage,<sup>3</sup> bone,<sup>4</sup> muscle,<sup>5,6</sup> and neural<sup>7</sup> tissue engineering, among others, as well as in anticancer therapies.<sup>8,9</sup>

Recently, interest has been shown in the incorporation of magnetic components into these polymeric matrices in order to produce magnetic 3D constructs for biomedical applications. Magnetic materials have shown great promise in this field due to their biocompatibility, both *in vitro* and *in vivo*; their remote controllability through the use of an external magnetic field, which reduces the need for invasive procedures and the associated risk in clinical setting; and their high adsorption capacity to the polymeric matrix, with applications in anticancer hyperthermia treatments and as contrast agents for medical imaging.<sup>10</sup> Furthermore, there have been reports of this type of approach being used as a tool to enhance the angiogenic potential of human umbilical vein endothelial cells (HUVECs), by triggering higher secretion of vascular endothelial growth factor (VEGF) by mesenchymal stem/stromal cells (MSCs) embedded in a magnetically-responsive scaffold.<sup>11</sup> MSCs have also been shown to overexpress VEGF after internalizing magnetic nanoparticles (MNPs)-laden liposomes in a mouse hind-limb ischemia model, resulting in higher revascularization,<sup>12</sup> as well as on their own when exposed to high-intensity pulsed electromagnetic fields.<sup>13</sup> Thus, the use of magnetic fields and components might have great implications in organ/tissue engineering, since vascularization is a major limitation in this field. Furthermore, the incorporation of magnetic components within an ink and 3D printing under external magnetic stimulation can be instrumental to obtain specific microarchitectures, potentially leading to a close mimicking of native tissues' structure and properties, namely allowing for collagen fibers orientations resembling the ones found in native cartilage.<sup>14</sup>

In this review, we provide an overview of recent studies performed on the field of magnetic hydrogels, with special emphasis on their manufacturing by 3D (bio) printing toward tissue engineering applications, which, to the best of our knowledge, has not yet been addressed in the literature. Firstly, we address the most commonly used techniques to fabricate MNPs and how they are incorporated into the hydrogels' matrices. As a result of the growing use of extrusion-based 3D (bio)printing strategies for the fabrication of magnetic hydrogels with complex microarchitectures, the basic concepts of this manufacturing technology are also detailed.

We also summarize the latest approaches in the 3D (bio)printing of magnetic hydrogels, highlighting their most promising results aiming at *in vitro* organ generation. Recent studies focused on the injectability of this type of hydrogels are also reviewed, given the importance of this feature for their use in 3D (bio)printing applications, more specifically following extrusion approaches. Finally, we discuss the current limitations of these strategies and how they can be overcome, and envision the applications of this technique in tissue and organ engineering.

## 2. Formulation of magnetic nanoparticles

The incorporation of magnetic particles into a polymeric matrix is the main strategy used when developing magnetic hydrogels for 3D (bio)printing applications. The application of an external magnetic field produces forces and torque in these particles, which then causes them to move, translationally or rotationally, dissipating energy. MNPs can be applied in the biomedical field as tools for drug delivery,<sup>15-17</sup> cancer therapy,<sup>15,18,19</sup> and medical imaging, among others.<sup>20</sup> Therefore, in this section, particular attention will be given to MNPs formulation and current applications.

MNPs have been drawing attention from the biomedical community due to their large surface-to-volume ratio, small size, good tissue diffusion, and easy manipulation via an external magnetic field.<sup>21</sup> Several different compositions have been studied, with the most reported and applied being the iron oxides magnetite ( $\text{Fe}_3\text{O}_4$ ) and maghemite ( $\gamma\text{-Fe}_2\text{O}_3$ ) due to their biocompatibility, superparamagnetism, and chemical stability at room temperature,<sup>21</sup> features that are advantageous for tissue engineering applications. Despite those properties, MNPs tend to aggregate due to their small size, in order to minimize their surface energy;<sup>21</sup> thus, different approaches have been proposed for the functionalization of these particles to improve their stability.<sup>6,9,22-28</sup> Moreover, unlike organic nanoparticles, MNPs present superior hyperthermic capabilities and can be easily visualized by magnetic resonance imaging techniques, making them ideal tools for medical imaging and applications in diagnosis.<sup>29</sup> Moreover, while gold nanoparticles (AuNPs) also present hyperthermic capabilities and can be used for imaging, MNPs still have the unique capability of being easily controlled remotely by the application of external magnetic fields.

MNPs production process includes a first step, where a short nucleation burst occurs due to the sudden addition of reagents and consequent reaction, which causes solution supersaturation and, thus, particle nuclei formation. Afterward, a second particle growth step takes place by continuous reaction of precursors with the existing particle

nuclei. At this stage, all the precursors added are consumed in particle growth, and no new nuclei are formed, as long as the rate of precursor reaction with the existing nuclei is higher than the rate of formation of new nuclei particles.<sup>30</sup> By controlling the rate of addition of precursors, it is possible to control the MNPs size distribution, achieving populations with low polydispersity indices.

Several strategies for the formulation of MNPs have been explored in the past few years in order to obtain MNPs with the desired features such as shape, size, magnetic controllability, and biocompatibility. These particles can be synthesized using physical and chemical methods, with some of the most reported ones being co-precipitation, thermal decomposition, and hydrothermal method.<sup>31</sup> Examples of these strategies are summarized in Table 1.

### 2.1. Co-precipitation

Co-precipitation is the most popular method to fabricate MNPs, since it is very straightforward and does not involve harmful precursors as in other fabrication methods.<sup>31</sup> Generally, it requires the dissolution of iron salts, with ferrous and ferric ions, which are then added to a basic solution at high or room temperature, causing the precipitation of the MNPs through a quasi-immediate crystallization that is greatly dependent on the electron exchange between  $\text{Fe}^{3+}$  and  $\text{Fe}^{2+}$  (Figure 1A).<sup>32</sup> The size and shape of the obtained particles depend greatly on various factors, such as pH, ionic ratio, temperature, type of salts used, and rate at which the solutions are mixed, among others.<sup>31</sup> Furthermore, the composition of the particles, whether they are composed of  $\text{Fe}_2\text{O}_3$ ,  $\text{Fe}_3\text{O}_4$ , or other iron oxides, also depends on the environmental conditions mentioned above.

This method, however, presents some limitations, such as the agglomeration of the nanoparticles during their fabrication, the need for careful control of the experimental factors of the reaction, such as temperature and pH, and the difficulties in creating a monodisperse and uniform population of MNPs.<sup>21</sup> This issue can be addressed through the functionalization of the formed particles, either by ligand addition/exchange or through particle encapsulation.<sup>33</sup> MNPs formulated by the co-precipitation method have been used in several areas of tissue engineering, namely for bone<sup>8,25</sup> and neural<sup>7</sup> regeneration strategies, anticancer hyperthermia therapies,<sup>34,35</sup> controlled drug release systems,<sup>34</sup> and providing antimicrobial properties.<sup>24</sup>

### 2.2. Hydrothermal method

The hydrothermal method (Figure 1B) is also another commonly used strategy for the fabrication of MNPs.<sup>36</sup> As described previously, metal salts are dissolved in water, which is followed by the addition of a basic solution until an alkaline pH is reached. Afterward, the mixture is placed

in a sealed container and kept at high temperature—130–250°C—and high pressure—0.3–4 MPa. Finally, the solution is filtered, and the solid components are dried and lyophilized, leading to the final product.<sup>31</sup>

This type of processing provides many advantages, such as the tailored MNPs morphology, which can present the shape of nanorods, nanotubes, nanosheets, and nanorings.<sup>31</sup> Moreover, the fabrication also allows to obtain a highly organized crystallite structure and does not employ organic solvents. However, this strategy is time-consuming due to its slow kinetics.<sup>36</sup> Hydrothermal methods have been used to fabricate magnetic nanoparticles for use in several biomedical applications, such as muscle<sup>6</sup> and cartilage<sup>37</sup> tissue engineering.

### 2.3. Thermal decomposition

Formation of MNPs by thermal decomposition starts with iron precursors being decomposed in high-temperature organic solvents, with surfactant stabilizers<sup>38</sup> in order to prevent the agglomeration of the formulated MNPs<sup>39</sup> (Figure 1C). This decomposition can happen following two processes: *heating-up* and *hot-injection*.<sup>40</sup> In the heating-up method, the pre-mixed precursor reagents, solvent, and surfactant stabilizers are heated to a certain temperature range. Temperatures in the range of 100–350°C have been shown to promote the formation of monodisperse particles with sizes between 4 nm and 30 nm.<sup>31</sup> In the hot-injection method, the growth phase is controlled by injecting the reagents into the hot surfactant solution,<sup>31</sup> causing burst nucleation.<sup>39</sup> Particles synthesized using the thermal decomposition method have been used in several biomedical applications, namely tumor ablation.<sup>9</sup>

Besides the option of synthesizing these particles in-house, MNPs are also commercially available, simplifying the process for the formulation of magnetic bioinks. These MNPs have been subjected to extensive quality control procedures, providing better reassurance of their performance in the desired applications. Some of the commercially available options are listed in Table S1 (Supplementary File).

## 3. Incorporation of MNPs in hydrogels

Magnetic hydrogels have been increasingly used in many fields of study due to their unique characteristics. MNPs can be incorporated into the hydrogels through three main methods: blending, grafting-onto method, and *in situ* precipitation.<sup>41</sup> These are summarized in Table 2.

### 3.1. Blending method

The blending method is the most commonly used method for the incorporation of MNPs into a hydrogel

Table 1. Examples of magnetic nanoparticles (MNPs) synthesized by different methods and their main properties and applications in tissue engineering and/or other therapeutic applications

Composition	Synthesis strategy	Functionalization/ Co-formulation	Main properties	Application	Ref.
Magnetite (Fe <sub>3</sub> O <sub>4</sub> )	None		S: 15 ± 1.2 nm M <sub>s</sub> : 49.24 emu/g M <sub>r</sub> : 0 emu/g	Nerve tissue engineering	7
			S: 8.62 ± 2.13 nm M <sub>s</sub> : 4.98 emu/g (max) M <sub>r</sub> : 0.22 emu/g	Bone tissue engineering • Hyperthermic therapy • Drug release	8
Magnetite (Fe <sub>3</sub> O <sub>4</sub> ) and γ-Fe <sub>2</sub> O <sub>3</sub>			Cluster size: ≈ 100 nm	Neuroendovascular reconstruction	89
Magnetite (Fe <sub>3</sub> O <sub>4</sub> )			S: 5–13 nm	Hyperthermic therapy	35
Magnetite (Fe <sub>3</sub> O <sub>4</sub> )	Co-precipitation		S: ≈ 10 nm	Magnetically-actuated hydrogels	22
			S: ≈ 10–20 nm M <sub>s</sub> : ≈ 60 emu/g	Soft robotics	23
Cobalt ferrite (CoFe <sub>2</sub> O <sub>4</sub> )		PAA	S: 9.2 ± 0.2 nm	• Antibacterial activity • Renal and hepatic toxicity assessment	24
			M <sub>s</sub> : 28.89 emu/g M <sub>r</sub> : 8.37 emu/g		
(1) Magnetite (Fe <sub>3</sub> O <sub>4</sub> ) (2) Cobalt ferrite (CoFe <sub>2</sub> O <sub>4</sub> )		Wrinkled mesoporous silica nanoparticles	S: 32.2 ± 4.3 nm (Fe <sub>3</sub> O <sub>4</sub> ), 33.6 ± 6.6 nm (CoFe <sub>2</sub> O <sub>4</sub> ) ZP: 25.1 mV (Fe <sub>3</sub> O <sub>4</sub> ), 22.3 mV (CoFe <sub>2</sub> O <sub>4</sub> )	Untested	90
Cobalt ferrite (CoFe <sub>2</sub> O <sub>4</sub> )		PVP	S: (25.45 ± 11.60) nm ZP: 12 mV	Bone tissue engineering	25
Magnetite (Fe <sub>3</sub> O <sub>4</sub> )		Oleic acid	S: 9 nm (functionalized), 13 nm (non-functionalized)	Angiogenesis	11
			Lysine	S: (13 ± 3) nm	<i>Escherichia coli</i> detection
γ-Fe <sub>2</sub> O <sub>3</sub>	Co-precipitation and solvothermal	PEG	S: ≈ 45–60 nm (w/PEG) ZP: -15.6 mV	Muscle tissue engineering	6
			S: 10–15 nm ZP: -32.72 ± 1.27 mV M <sub>s</sub> : 62.8 emu/g M <sub>r</sub> : 1.4 emu/g	Cartilage tissue engineering	37
Magnetite (Fe <sub>3</sub> O <sub>4</sub> )	Thermal decomposition	Phosphorylated mPEG	S: 33 nm	Antitumor therapy	27
			M <sub>s</sub> : 48.2 emu/g M <sub>r</sub> : 0 emu/g		
Cobalt ferrite (CoFe <sub>2</sub> O <sub>4</sub> )	Thermal decomposition	None	S (core): 10.1 ± 1.1 nm S (whole): 15.6 ± 2.3 nm M <sub>s</sub> : ≈ 35 emu/g M <sub>r</sub> : 0 emu/g	Untested	92
			DSPE-PEG2000	S: ≈ 30–40 nm	Tumor ablation
Cobalt ferrite (CoFe <sub>2</sub> O <sub>4</sub> )	Thermal decomposition	None	S: ≈ 20 nm	Untested	93,94
			M <sub>s</sub> : 52.35 emu/g M <sub>r</sub> : 8.3–14.40 emu/g		

Abbreviations: CoO, cobalt(II) oxide; DSPE-PEG2000, 1,2-distearoyl-sn-glycero-3-phosphoethanolamine-N-[methoxy(polyethylene glycol)-2000]; mPEG, poly (ethylene glycol)-methoxy; M<sub>r</sub>, remanent magnetization; M<sub>s</sub>, saturation magnetization; PAA, poly(acrylic acid); PVP, poly(vinylpyrrolidone); S, average size; ZP, Zeta potential.

Table 2. Examples of magnetic hydrogels manufactured through conventional techniques

Hydrogel (type)	Composition of MNPs	Incorporation technique	Applications	MNP characteristics	Stability of the MNPs in the matrix	Ref.
Silk fibroin (N)			Tumor ablation	S: $\approx$ 30–40 nm C: 0.5, 1, and 2 mg/mL Homogeneous distribution	Not studied	9
Fibrin-agarose (N)			Cartilage tissue engineering	S: 110 nm C: 0.1% (v/v)	Not studied	27
Alginate and MC (SSy)	Magnetite ( $Fe_3O_4$ )		Magnetically-actuated hydrogels	S: $10.01 \pm 2.23$ nm C: $\approx$ 15% (w/w) Homogeneous distribution	Stable due to the PAA interactions with water	22
CMCS and OGG (SSy)			Soft robotics	C: 0, 10, and 20% (w/v) Homogeneous distribution	Stable due to PAA interaction with matrix	23
			<ul style="list-style-type: none"> <li>Bone tissue engineering</li> <li>Drug delivery</li> </ul>	S: 10–20 nm C: $\approx$ 5, 10, and 20 mg/mL	Stable	4
			Antibacterial activity	C: 100, 200, and 500 $\mu$ g/mL	Not studied	58
GelMA (SSy)	$\gamma$ - $Fe_2O_3$	Blending	Muscle tissue engineering	S: $\approx$ 45–60 nm (with PEG) C: 0.3 mg/mL Homogeneous distribution (without magnetic field alignment)	Stable	6
OHA, GC, and ADH (SSy)	Magnetite ( $Fe_3O_4$ )		Cartilage tissue engineering	S: $\approx$ 20 nm C: 1, 3, and 5 wt%	Not studied	3
PVA, NaAlg, and Hap (SSy)			Bone tissue engineering	C: 5, 10, and 15% (MGO) Homogeneous distribution	Stable	8
CMHPG (SSy)	Cobalt ferrite ( $CoFe_2O_4$ )		Magnetically-actuated hydrogels	S: 20 nm C: 0–10% (w/w) Homogeneous distribution	Stable	95
CEC and AHA (SSy)	Carbonyl iron (CFeO)		Controllability of magnetic scaffolds	S: 1.26 $\mu$ m C: 0.1 and 0.5 w/v% Homogeneous distribution (without magnetic field alignment)	Not studied	45
Chitosan (N)			Hypothermia	S: 5–13 nm	Dependent on the crosslinking density	35
Bacterial nanocellulose (N)		<i>In situ</i>	Neuroendovascular reconstruction	Cluster S: $\approx$ 100 nm	Not studied	89
PAMPS/PAAm (Sy)			<ul style="list-style-type: none"> <li>Tissue hyperthermia</li> <li>Drug release</li> </ul>	S: $(8.62 \pm 2.13)$ nm CV: 24.7%	Not studied	34
PAAm coated with PDMS (Sy)	Magnetite ( $Fe_3O_4$ )	Grafting-onto	Muscle tissue engineering Implantable medical devices	S: $\approx$ 200 nm C: up to 60% (w/w) Homogeneous distribution	Stable given that they are integrated within the polymeric network	46
Alginate (N)		Blending of magnetic nanofibers	Nerve tissue engineering	S: $(15 \pm 1.2)$ nm C: 10% w/w of fiber: polymer	Not studied	7
GelMA (SSy)			Muscle tissue engineering	S: 20–30 nm C: 20 mg/mL (in the fibers) Homogeneous distribution (fibers)	Not studied	5

Abbreviations: ADH, adipic acid dihydrazide; AHA, aldehyde hyaluronic acid; C, concentration; CEC, N-carboxyethyl chitosan; CMCS, carboxymethyl chitosan; CMHPG, Carboxymethyl hydroxypropyl guar; GC, glycol chitosan; GelMA, gelatin methacryloyl; HAp, hydroxyapatite; MC, methylcellulose; N, natural polymer; NaAlg, sodium alginate; OGG, oxidized gellan gum; OHA, oxidized hyaluronate; PAA, poly(acrylic acid); PAAm, polyacrylamide; PAMPS, poly(2-acrylamido-2-methylpropane sulfonic acid); PDMS, polydimethylsiloxane; PVA, poly(vinyl alcohol); S, average size; SSy, semisynthetic polymer; Sy, synthetic polymer.

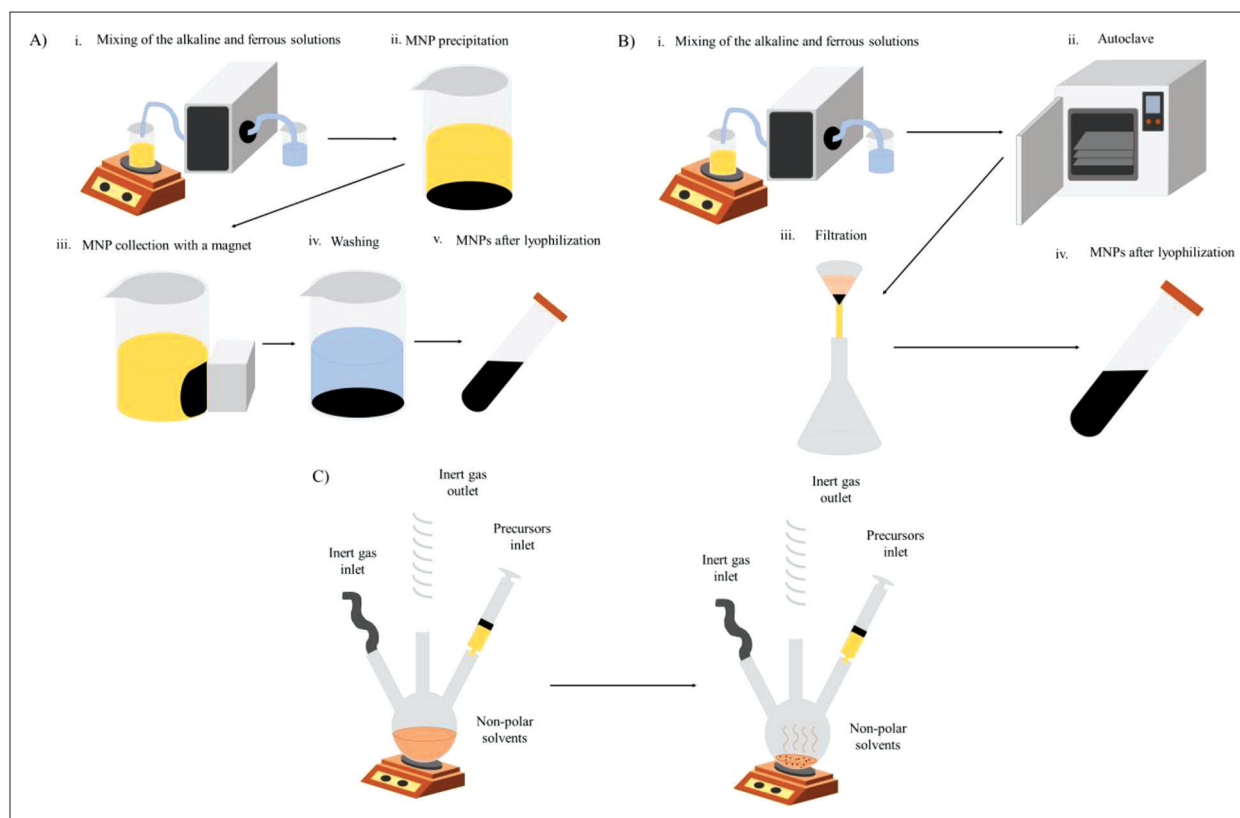


**Figure 1.** Summary of the MNP synthesis techniques. (A) Co-precipitation: a basic solution is added to a solution with ferrous ions (i), inducing the precipitation of MNPs (ii) that are then attracted to a magnet (iii), washed (iv), and lyophilized (v). (B) Hydrothermal method: a basic solution is added to a solution with ferrous ions (i). The resulting solution is kept in an autoclave at high temperature and pressure (ii) to control the formation of MNPs, which are then filtered (iii), dried, and pulverized (iv). (C) Thermal decomposition (*heating-up*): precursor reagents are mixed under an inert gas atmosphere at high temperatures, under reflux; after heating the mixture to the boiling point of the solvent and the decomposition point of the precursors, crystals form and, after a growth phase, the MNPs are obtained.

polymeric matrix due to its convenience and procedural simplicity. In this approach, the MNPs are prepared separately from the hydrogel and are then dispersed in the pre-crosslinked hydrogel solution, often resorting to sonication to achieve good dispersion in the solution (Figure 2A).

Despite the advantages of this approach, the fact that the particles are not strongly bound to the polymeric chains can cause them to diffuse out of the hydrogel,<sup>42</sup> as well as lead to an uneven particle distribution throughout the polymeric matrix.<sup>10</sup> Furthermore, the particles can aggregate, which is generally unwanted in biomedical applications, potentially lead to toxicity,<sup>43</sup> and affect their efficiency, for example, decreasing their hyperthermic ability, which is very important for cancer therapies.<sup>44</sup> This type of approach has been used in various studies, to obtain magnetic hydrogels targeting several purposes, such as the fabrication of anisotropic structures,<sup>45</sup> drug delivery systems, and bone tissue engineered structures<sup>4</sup> as well as the optimization of

bioink composition for bioprinting of magnetically-responsive structures.<sup>22</sup>

### 3.2. Grafting-onto method

In the grafting-onto method, MNPs are also embedded in the hydrogel solution before the crosslinking process takes place. However, in this method, functional groups are grafted onto the particles prior to their mixing with the solution<sup>41</sup> (Figure 2B). These functional groups then interact with the polymeric chains of the hydrogel during crosslinking, working to create bonds with the hydrogel, and thus MNPs become an integral part of the overall structure.

This technique allows for a more uniform dispersion and better stability of the MNPs within the polymeric matrix. Nevertheless, the functionalization of the nanoparticles is very time-consuming, costly, and complex.<sup>41</sup> This method was reported by Hu *et al.*<sup>46</sup> who fabricated adhesive, tough, and strong polyacrylamide hydrogels, with a concentration of MNPs as high as 60%,

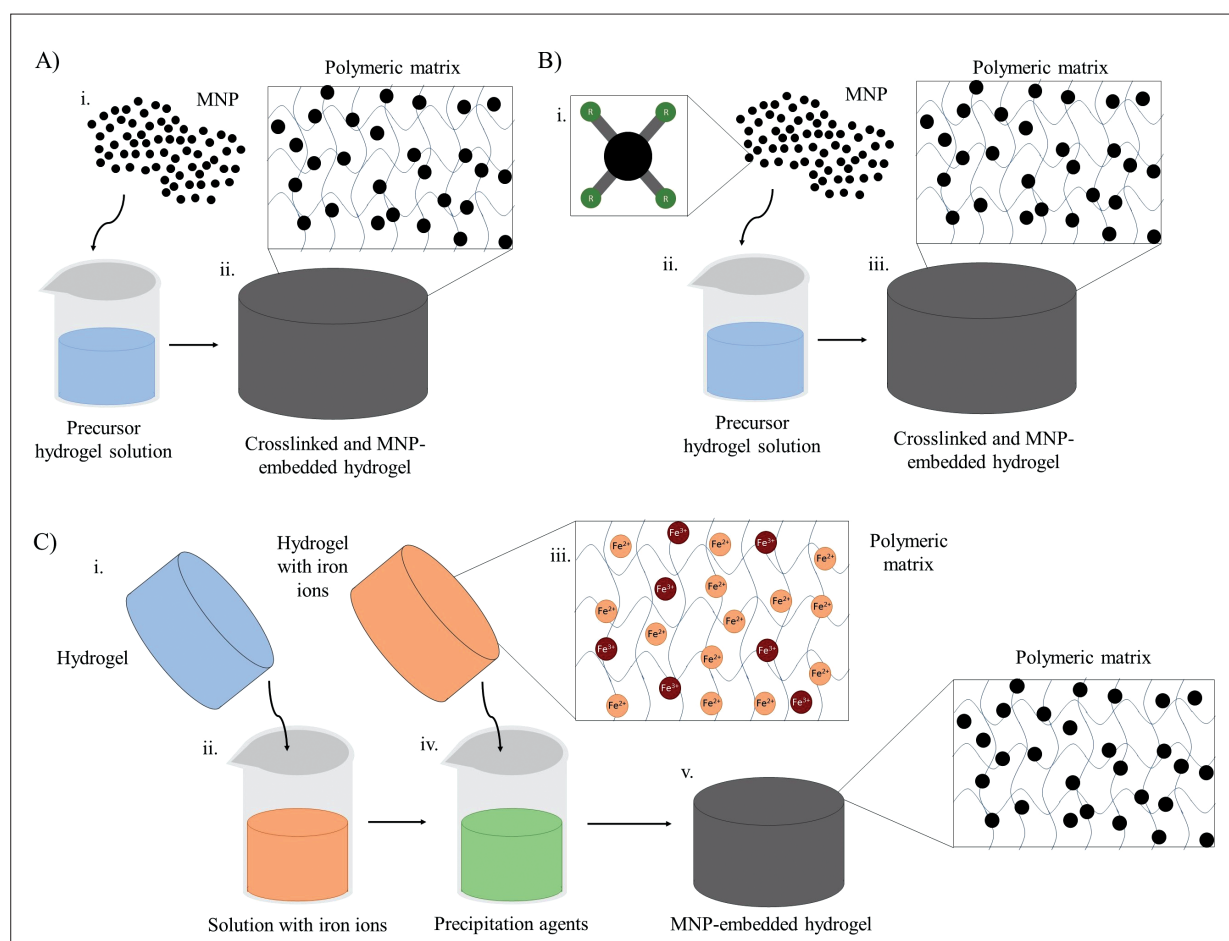


**Figure 2.** Overview of the techniques for the incorporation of MNPs in hydrogels. (A) Blending method: MNPs are blended in the pre-crosslinked hydrogel (i), which is then crosslinked (ii), with the particles being embedded in the matrix. (B) Grafting-onto method: the functionalized MNPs (i) are mixed with the pre-crosslinked hydrogel (ii), which is then crosslinked (iii) with MNPs being an integral part of the network. (C) *In situ* method: the crosslinked hydrogel (i) is dipped into a solution with iron ions (ii), which diffuse into the matrix (iii) and then put in contact with precipitating agents (iv), promoting the formation of MNPs (v).

achieving a high stability of hydrogel after the MNPs were integrated into the matrix's structure.<sup>46</sup>

### 3.3. *In situ* precipitation

In this method, hydrogels are crosslinked prior to the incorporation of the magnetic component and subsequently immersed in a solution containing  $\text{Fe}^{3+}$  and  $\text{Fe}^{2+}$  ions (Figure 2C). This allows them to disperse throughout the entire hydrogel's network in a uniform manner<sup>47</sup> and then precipitate, resulting in the formation of MNPs. Despite allowing for a better entrapment of the particles within the hydrogel, the use of harsh precipitation agents might limit this approach's compatibility with natural biomaterials and cells,<sup>42</sup> restricting its use to materials that can withstand these agents without getting degraded.<sup>41</sup>

This technique has been used by Miyazaki *et al.*,<sup>35</sup> who developed a chitosan hydrogel by *in situ* precipitation of magnetite nanoparticles in order to assess their heat-

generating abilities.<sup>35</sup> Additionally, Tang *et al.*<sup>34</sup> also created a poly(2-acrylamido-2-methylpropane sulfonic acid)/polyacrylamide hydrogel with the same type of nanoparticles. This hydrogel presented hyperthermic properties when exposed to an external magnetic field in four different types of porcine tissue, both in solution and exposed to air. Moreover, the magnetic hydrogel effectively promoted a controllable and sustained drug release.<sup>34</sup>

## 4. 3D (bio)printing of magnetic hydrogels

This section provides a brief description of 3D extrusion printing, which is the additive manufacturing technique more commonly used for printing magnetic hydrogels aiming at tissue engineering applications. 3D extrusion bioprinting is a nomenclature only reserved for approaches where live cells are incorporated inside the inks, while 3D extrusion (bio)printing is a broader nomenclature applied

for inks that may or not contain cells. An overview on selected recent studies exploring approaches for 3D (bio) printing of magnetic hydrogels is provided.

#### 4.1. 3D extrusion bioprinting

3D (bio)printing is a technique that allows the manufacturing of 3D, well-organized structures by applying layer-by-layer precise positioning of biomaterials, biomolecules (e.g., growth factors<sup>48</sup>), and/or cells. This technique allows fabrication of constructs with different biological and mechanical biomimicking features naturally found in the target tissue, with potential applications in tissue engineering,<sup>49</sup> drug delivery,<sup>50</sup> or in the development of organs on chips for disease modeling and drug screening.<sup>51</sup> In this review, special attention is given to extrusion, the technique most predominantly reported to 3D (bio)printing of magnetic hydrogels. Additional information on inkjet and laser assisted-bioprinting methods can be found elsewhere.<sup>49,52-54</sup>

3D extrusion bioprinting relies on pushing a bioink through a syringe by either pneumatic or mechanical methods,<sup>49</sup> to produce a filament which is placed, layer by layer, in a specific shape, according to a model designed using computer-aided design (CAD) software. The bioink is composed by one or more biomaterial, cells, and, potentially, other biomolecules to aid in cell function and/or proliferation. These must be biocompatible and have mechanical, rheological, chemical, and biological characteristics that allow to produce a final structure that resembles the tissue mechanics and structure, with high shape fidelity to the intended design and low batch-to-batch variation.<sup>55</sup>

The main advantages of extrusion bioprinting, when compared to other advanced manufacturing techniques, are its affordability<sup>56</sup> and its ability to print bioinks with high cell densities and to extrude more viscous solutions,<sup>57</sup> which allow for a diverse array of materials to be used in bioinks formulation. While cell viability can be affected by the high shear stresses the cells are subjected to,<sup>49</sup> 3D extrusion bioprinting has been studied in several areas of tissue engineering.<sup>3,6,8,22,23,58</sup>

#### 4.2. Applications of 3D (bio)printed magnetic hydrogels

3D (bio)printing of magnetic hydrogels experienced a growing interest for the manufacturing of smart and structure-defined scaffolds for tissue engineering applications. Magnetically-responsive materials used for this purpose need to be compatible with the printing process, namely in terms of rheological properties, gelation kinetics, and crosslinking nature.<sup>59</sup> Furthermore, printing parameters such as printing resolution and shape fidelity also affect the final characteristics of the hydrogels. These

hydrogels should be biocompatible and present adequate bioactive cues, mechanical properties, and degradation profiles that mimic those of the target tissue<sup>59</sup> according to whether the construct is supposed to replace the tissue or support the regeneration process. Several examples of hydrogels fabricated using 3D (bio)printing and of other types of constructs obtained through this manufacturing process are summarized in Table 3 and Figure 3.

##### 4.2.1. Cartilage tissue engineering

Magnetic hydrogels are applied to cartilage tissue engineering strategies. Magnetic nanoparticles can increase the chondrogenic differentiation potential of cells through various mechanisms, namely upon internalization by the cells, by binding to their surface or serving as a guide for their migration and condensation in one single location,<sup>60</sup> which is crucial in cartilage formation. However, the application of these hydrogels in this field is very challenging given that cartilage tissue has a highly complex structure, and the proper combination of specific biochemical/physical cues is required to achieve functional tissue substitutes. Indeed, a method to produce such cartilage substitute with native-like extracellular matrix composition and adequate mechanical properties has not yet been developed. 3D (bio)printing of magnetic hydrogels has the potential to construct a structure that more closely resembles the native cartilaginous tissue by accurately mimicking its natural architecture,<sup>61</sup> which can then be combined with an external magnetic stimulation to further stimulate the scaffold's microenvironment in a remote and non-invasive manner.<sup>60</sup>

In an attempt to mimic this specific microenvironment, Betsch *et al.*<sup>14</sup> explored the insertion of time as a fourth dimension in the bioprinting process of magnetic hydrogels aiming to generate two-layered constructs, each with a different fiber arrangement (aligned or random), built sequentially according to a time-dependent orientation of the magnetic field. To achieve this goal, the authors used an agarose and type I collagen blend with streptavidin-coated iron nanoparticles to improve the particles' attachment to the collagen fiber network. The results showed that the collagen fibers, within the scaffold, are aligned in parallel to the magnetic field due to the movement of the particles. Furthermore, the alignment of the fibers led to an increase in the compression moduli of the scaffolds. Human knee articular chondrocytes were seeded on the two-layered scaffolds, one layer with horizontally aligned fibers and the other with randomly oriented fibers, mimicking the superficial and middle layers of articular cartilage tissue, respectively. The results showed that the scaffolds were cytocompatible, and the expression of collagens I and II by the cells cultivated on the two-layered scaffolds was

Table 3. Examples of studies using 3D printing/bioprinting approaches for the fabrication of magnetic hydrogels

Magnetic component	Hydrogel constitution	Cell type	Target applications	Physicochemical features	Biological outcomes	Ref.
SPIONs	OHA, GC and ADH	ATDC5 (chondrogenic)		<ul style="list-style-type: none"> <li>Self-healing behavior,</li> <li>SPIONs decreased mechanical properties.</li> </ul>	<ul style="list-style-type: none"> <li>Good cell viability,</li> <li>Increased SOX9 and COL-2 gene expression due to magnetic stimulation.</li> </ul>	3
Magnetite (Fe <sub>3</sub> O <sub>4</sub> )	Alginate and MC	hMSCs	Cartilage tissue engineering	<ul style="list-style-type: none"> <li>Smooth extrusion up to 30% of particles,</li> <li>YM increased with the increase of particle concentration.</li> </ul>	<ul style="list-style-type: none"> <li>High cell viability.</li> </ul>	64
Streptavidin-coated IONPs	Agarose and type I collagen	hKAC		<ul style="list-style-type: none"> <li>Coating of IONPs allowed better adhesion to collagen,</li> <li>Aligned collagen led to increased compression moduli.</li> </ul>	<ul style="list-style-type: none"> <li>High cytocompatibility,</li> <li>Good mimicking of two different layers of cartilage.</li> </ul>	71
MGO	PVA, NaAlg and HAP	Mouse BMSCs	Bone tissue engineering; tumor ablation	<ul style="list-style-type: none"> <li>Pore size conducive to cell growth and nutrient transportation,</li> <li>MGO improved the scaffold's thermal stability.</li> </ul>	<ul style="list-style-type: none"> <li>MGO enhanced cell adhesion and Osteogenic differentiation,</li> <li>High biocompatibility,</li> <li>Hyperthermic effects in tumor-bearing mice.</li> </ul>	8
PAA-MNPs	Alginate and MC	Not used	Magnetically-actuated hydrogels	<ul style="list-style-type: none"> <li>Increased hydrogel responsiveness and compressive strength with increasing MNP content.</li> <li>MNPs induced hydrogel deformation upon magnetization.</li> <li>MNPs increased shear-thinning behavior.</li> </ul>	None	22
IOPs and PEG-IOPs	GelMA	hMSCs and C2C12 (mouse myoblast)	Muscle tissue engineering	<ul style="list-style-type: none"> <li>Alignment of IOPs increased mechanical properties,</li> <li>Construction of a magnetically controlled structure.</li> </ul>	<ul style="list-style-type: none"> <li>Cells aligned according to the IOPs filaments,</li> <li>Enhanced myotube organization.</li> </ul>	6
SPIONs		HUVEC and NIH3T3 fibroblast cell line	Antibacterial activity	<ul style="list-style-type: none"> <li>MNPs decreased the compressive modulus</li> </ul>	<ul style="list-style-type: none"> <li>SPIONs are cytocompatible,</li> <li>Formation of an endothelium-like structure,</li> <li>Antibacterial activity.</li> </ul>	58
Iron oxide	Silk-GMA and Gelatin-GMA	C2C12 (mouse myoblast)	Muscle tissue engineering	<ul style="list-style-type: none"> <li>Tensile and compressive strength increased with increasing particle content</li> <li>Different structures were printed and functional,</li> <li>Behavior of hydrogels depended on the layers' organization,</li> <li>MNPs decreased the viscoelastic modulus.</li> </ul>	<ul style="list-style-type: none"> <li>Cells aligned according to hydrogel stretching improved myotube characteristics.</li> </ul>	71
PAA-MNPs	Alginate and MC	L929 fibroblasts	Soft robotics		<ul style="list-style-type: none"> <li>High cell viability</li> </ul>	23

Abbreviations: ADH, adipic acid dihydrazide; BMSCs, bone marrow-derived mesenchymal stromal cells; GC, glycol chitosan; GMA, glycidyl methacrylate; GelMA, gelatin methacryloyl; HAP, hydroxyapatite; hMSCs, human mesenchymal stromal cells; hKAC, human knee articular chondrocytes; HUVEC, human umbilical vein endothelial cells; IONPs, iron oxide (nano)particles; MC, methylcellulose; MGO, magnetic graphene oxide; NaAlg, sodium alginate; OHA, oxidized hyaluronate; PAA-MNP, poly(acrylic acid)-functionalized magnetic nanoparticles; PCL, polycaprolactone; PEG-IOPs, poly(ethylene glycol)-functionalized IOPs; PVA, poly(vinyl alcohol); SPION, superparamagnetic iron oxide nanoparticles; YM, Young's modulus.

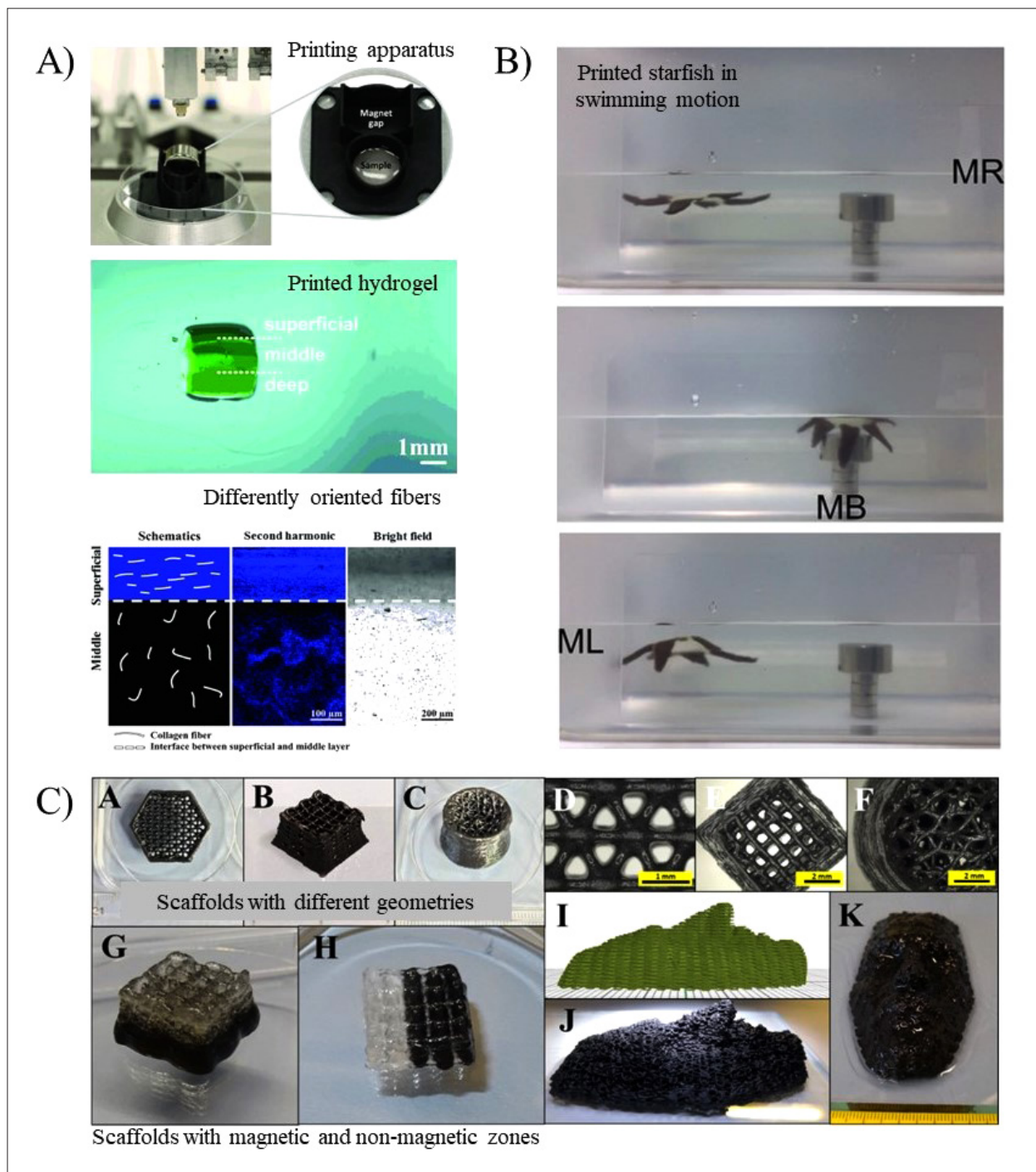


**Figure 3.** Examples of applications of magnetic hydrogels fabricated using 3D (bio)printing techniques. This approach allows to tailor the architecture of fibers within printed hydrogels while they are being printed (in (A) top to bottom: printing apparatus with magnetic stimulation, printed hydrogel with differently oriented fibers, and microarchitecture of the different layers of the hydrogel). This approach has applications in the printing of controllable soft robots for tissue engineering applications (B) and allows the creation of very complex and diverse structures, such as the nose of Nikola Tesla (in (C): I–K). Reproduced with permission from [14], [6], and [64], respectively. Abbreviations: MR, right magnet; ML, left magnet; MB, bottom magnet.

higher than the ones cultured on scaffolds consisting of only one of the two layers. The obtained results highlight the importance of the microarchitecture of the scaffold, and the strategy followed in this work shows how magnetic stimulation and 3D (bio)printing can both be synergistically combined to recreate more native-like structures. Nonetheless, the inkjet printing approach used in such work is most suitable for printing low-viscosity solutions,<sup>62</sup> which narrows the list of biomaterials to be used, limits the cell concentration that can be deposited, and when applied to thicker and complex 3D geometries, may result in structures that are not able to sustain their physical integrity.<sup>63</sup> Such limitation can be overcome by resorting to extrusion bioprinting approaches.

Another strategy to manipulate chondrocyte phenotype using magnetic stimulation has been explored by Choi *et al.*,<sup>3</sup> who developed a hydrogel made from oxidized hyaluronate, glycol chitosan, adipic acid dihydrazide, and superparamagnetic iron oxide nanoparticles (SPIONs), and tested the printability of the bioink using an extrusion 3D bioprinter. The cell viability and the chondrogenic differentiation of ATDC5 cells *in vitro* were also assessed. The results obtained showed that the introduction of SPIONs in the matrix led to a decrease in the mechanical properties of the hydrogel, corresponding to a decrease in its storage modulus, while cell viability was not affected by the magnetic stimulation, SPIONs, or the 3D bioprinting process itself. The application of magnetic fields to the tissue constructs obtained also resulted in an increase in the expression of *SOX9* and *COL2* genes, suggesting a positive effect on chondrogenic differentiation.

In a different study, Spangenberg *et al.*<sup>64</sup> formulated a hydrogel composed of alginate and methylcellulose (algMC) with embedded magnetite microparticles. The authors observed that a condition with 25% w/w of embedded particles in the hydrogel showed appropriate rheological properties, allowing for a smooth ink extrusion, magnetization, and printability. An increase in the scaffolds' Young's modulus was also observed following the addition of particles, with the 25% w/w of particles hydrogel formulation presenting values similar to the ones described for the native cartilage tissue, at values of  $627 \pm 53$  kPa and  $1.03 \pm 0.48$  MPa, respectively.<sup>65</sup> Cytocompatibility assays performed using an immortalized MSC cell line showed that cells cultured in a plain algMC scaffold presented a slightly decreased initial cell viability, which however increased over the 21 days in culture.

An alginate and methylcellulose (MC) hydrogel containing embedded poly(acrylic acid) (PAA) stabilized-MNPs (PAA-MNPs), mixed at different ratios, was developed by Podstawczyk *et al.*<sup>22</sup> The addition of the PAA-MNPs led

to increased viscosity and enhanced shear-thinning effects on the precursor ink. This study demonstrated that a higher PAA:MNP ratio led to a better quality of the 3D-printed structures. The application of a magnetic field decreased the equilibrium swelling degree of the scaffolds and caused a deformation of the microstructure in its direction. Therefore, these works show the need to optimize ink formulations in order to achieve the desired outcomes concerning printability, biocompatibility, and magnetic response, paving the way for the application of magnetically-responsive hydrogels in cartilage tissue engineering strategies. Importantly, the hydrogel formulation should be tested in terms of its ability to promote cell viability, proliferation, and chondrogenic differentiation.

#### 4.2.2. Bone tissue engineering

Hydrogels are usually not used as materials to substitute bone due to their lower mechanical stiffness in comparison with this type of hard tissue. Still, magnetic hydrogels can be used in bone tissue engineering as vehicles to induce regeneration of bone defects.<sup>66</sup> The introduction of magnetic components within scaffolds for bone tissue engineering can allow the creation of an anisotropic identity characteristic of this type of tissue, as well as increase the mechanical stiffness of hydrogels that would otherwise be too soft for this application.<sup>67</sup> Furthermore, a 3D (bio)printing approach can allow for a more precise replication of bone's native porous microarchitecture.<sup>68</sup>

Targeting potential bone tissue engineering applications, Li *et al.*'s work<sup>8</sup> focused on the 3D extrusion printing of a hydrogel consisting of a mixture of polyvinyl alcohol, sodium alginate, and hydroxyapatite (PVA/SA/HA) with graphene oxide functionalized with iron nanoparticles (magnetic graphene oxide, MGO). Similar to previous studies, the authors concluded that the incorporation of hydroxyapatite in the structure improved the mechanical properties of the scaffold, and that the addition of MGO had beneficial effects in cell adhesion without any cytotoxicity effects. The ability of the scaffolds to promote the osteogenic differentiation of rat bone marrow-derived MSCs (BMSCs) or to inhibit tumor growth through hyperthermia *in vivo* was also analyzed. These results highlight the potential application of these scaffolds both in bone regeneration and tumor targeting strategies. Nevertheless, it is worth noting that in this study the printing process did not contain cells embedded in the ink, which could be a valuable addition to the performance of the hydrogel *in vivo* via, for example, secretion of growth factors that would further enhance bone regeneration.

#### 4.2.3. Muscle tissue engineering

Muscle tissue engineering has also been explored as an application in which magnetic hydrogels can play a role.

When combined with hydrogels, MNPs can promote cell alignment upon magnetic stimulation, which is advantageous to mimicking the native muscle tissue anisotropy.<sup>69</sup> Moreover, the ability to respond to an external magnetic field allows the simulation of muscle contraction, meaning that these materials can potentially be used as artificial muscles.<sup>67</sup>

To address the ability of magnetically-responsive hydrogels to respond to external stimuli, Tognato *et al.* fabricated a cell-laden anisotropic gelatin methacryloyl (GelMA) hydrogel that could change its conformation when stimulated.<sup>6</sup> The hydrogel was formed through the application of an external magnetic field of very low intensity (0.02 T), which induces orientation of the iron oxide nanoparticles (IOPs), followed by exposure to ultraviolet (UV) light for further crosslinking. The authors claimed that it is possible to tune the size and length of IOP filaments, as well as the distance between filaments. Cell seeding and encapsulation assays were performed using human BMSCs and C2C12 mouse myoblast cells, respectively. The authors observed that using aligned IOP filaments promoted the orientation of both types of cells in the IOP filaments direction, and C2C12 cells encapsulation on these hydrogels resulted in an increased number of mature multinucleated myotubes. These results show that the recapitulation of the fiber alignment of native muscle tissue is possible in an *in vitro* setting. Furthermore, there are already existing reports on the bioprinting of a GelMA bioink containing C2C12 cells which achieved good cell viability (> 90%) even after UV exposure.<sup>70</sup> These results mean that these cells can withstand the stress of the extrusion procedure and the posterior crosslinking reaction, showing the potential of the 3D (bio)printing of a magnetic bioink for this application.

In order to stimulate a cell-laden hydrogel to modulate their morphology and differentiation, Ajiteru *et al.*<sup>71</sup> used an interesting approach by developing a magnetic bioreactor. The authors fabricated a hydrogel composed of two different layers: one made from glycidyl methacrylated silk fibroin (Silk-GMA) with incorporated iron oxide particles, and another made from gelatin glycidyl methacrylate (Gel-GMA) with incorporated C2C12 cells. After stimulation in the magnetic bioreactor, the authors observed that the Silk-GMA + 7% iron oxide particles actively responded to the magnetic force similarly until the end of the 8-day experiment. In this assay, the myoblasts aligned in the direction of the magnetic stretching to which the hydrogel was exposed by two-axis and four-axis bioreactor systems. The bioreactor system promoted the formation of multinucleated myotubes with increased myotube diameter and length, and enhanced the expression of myogenic markers such as Pax7, MyoG, and TnnT1. The

use of this bioreactor system allowed the stimulation of the hydrogel while it was being fabricated, thus permitting a closer control of the structure's manufacture.

Adding MNPs to hydrogels has great implications in muscle tissue engineering, since it allows for a close control over their motion within the scaffold, as well as provides the hydrogel structure with shape memory capabilities.<sup>72</sup> 3D (bio)printing is also a valuable approach to this field, since it allows to precisely deposit material that can, for example, mimic the fascicular structure of skeletal muscle tissue<sup>73</sup> or to fabricate heart patches for cardiac regeneration.<sup>74</sup> Thus, the combination of these two strategies is a path that can bring significant advances to the area.

#### 4.2.4. Other applications

Magnetic hydrogels can also have antibacterial activity. The MNPs embedded within the polymeric matrix can potentially induce bacterial death through various mechanisms, namely electrostatic interactions with the cell membrane, potentially disrupting it and causing the leakage of cytoplasmic components. Furthermore, it has been suggested that there is a higher level of reactive oxygen species (ROS) formed on the surface of the MNPs, with these ROS playing a major role in the destruction of cellular components such as proteins and DNA. Another path that can cause bacterial death involves a photocatalytic effect that occurs when MNPs are stimulated with visible light, inducing changes in their electronic structure and originating free electrons, that can induce formation of ROS and cause cell death.<sup>75</sup> Despite all these potential paths to cell death, bactericidal effect of MNPs is executed mainly through ROS production, chlorosis, and hypoxia.<sup>76</sup> This type of approach is especially relevant in countering antibiotic-resistant microorganisms<sup>77</sup> or preventing infections post-implantation by providing a non-invasive and non-harmful solution.

Accordingly, Theus *et al.*<sup>58</sup> fabricated a GelMA scaffold embedded with SPIONs through a 3D printing process and tested its effects on cell viability and its antibacterial properties. The authors concluded that the incorporation of SPIONs in the bioink led to a decrease in the compression modulus of the hydrogel, which was attributed to the blocking of bonds that could be formed upon crosslinking within the backbone of the polymer. Cell viability was assessed by culturing two different cell lines, HUVEC and NIH3T3 (a fibroblast cell line), in the presence of SPIONs both in two-dimensional and 3D environments. The results showed that the hydrogel had high biocompatibility. Furthermore, scaffolds containing SPIONs showed enhanced antibacterial activity against *Staphylococcus aureus*, with such activity increasing with an increase in the concentration of SPIONs present in the system.

Magnetic hydrogels may be employed in soft robotics due to their remote controllability. These actuators mainly function through the shape change that is induced by an external magnetic field, which exerts a force in the MNPs which, in turn, is transmitted to the polymeric matrix.<sup>78</sup> Moreover, the 3D printing process allows the fabrication of magnetic hydrogels of various shapes; therefore, this method can be applied to produce soft robots for different purposes.

In order to test the ability of a 3D printing strategy to build complex and magnetically-responsive structures, Simińska-Stanny *et al.* printed alginate and methylcellulose hydrogels containing a gradient of PAA-stabilized MNPs, into various shapes such as wheels, cantilevers, or cubes.<sup>23</sup> The ink possessed a shear-thinning behavior due to the presence of methylcellulose, and this behavior was enhanced by the introduction of MNPs in the system, even though it caused a decrease in the viscoelastic modulus of the ink. The printed structures could be remotely controlled through the application of an external magnetic field, and this control depended on the organization of the layers within the hydrogel. Regarding cell viability, L929 fibroblasts were able to maintain an adequate viability in the magnetic hydrogels (>85%), demonstrating the biocompatibility of this material. Besides their efforts in fabricating hydrogels for muscle tissue engineering applications, Tognato *et al.* also reported the use of a GelMA ink to 3D-print a soft robot in the shape of a starfish whose flapping motion could be guided by external alternating magnetic fields. These experiments prove that using magnetic hydrogels for the control of constructs can elicit an effect in the body when exposed to external magnetic fields.<sup>6</sup>

## 5. Injectable magnetic hydrogels and their potential use in 3D (bio)printing

One of the main characteristics for an hydrogel to be eligible for 3D (bio)printing purposes is its ability to be injected through a nozzle: not only must the hydrogel possess rheological properties that allow it to hold its shape after printing, but it also must possess an adequate interface compatibility with the nozzle's material, so as not to increase the pressure needed to extrude it nor to cause an augmented shear stress that can, subsequently, reduce cell viability within the printed scaffold.<sup>79</sup> Thus, research in the injectability of hydrogels has direct impact in their potential to be used in 3D (bio)printing strategies. With this in mind, this section summarizes some of the recent advances made in the fabrication of injectable magnetic hydrogels.

Self-healing hydrogels are quite appealing for 3D (bio) printing. This type of hydrogels can recover their structure

after having been exposed to external forces through dynamic covalent crosslinking or covalent and non-covalent interactions.<sup>80</sup> These features make them very interesting materials for tissue engineering applications since they can extend the materials' longevity while maintaining their original characteristics.<sup>80</sup>

Using a mixture of N-carboxyethyl chitosan (CEC) and aldehyde hyaluronic acid (AHA), Nardecchia *et al.* formulated an injectable bioink loaded with magnetic particles to introduce anisotropy in a construct through the application of external magnetic fields.<sup>45</sup> The mixture of these compounds led to the formation of Schiff base—compounds possessing a double bond connecting a carbon and a nitrogen atom<sup>81</sup>—bonds between amino groups of CEC and aldehyde groups of AHA. The results of this study showed that the magnetic particles aligned themselves in the direction of the magnetic field, and that they improved the strength of the overall matrix. Additionally, there was also evidence that hysteresis could be controlled via an external magnetic field, which enables the tuning of the mechanical properties of the hydrogel once it has been injected. The same type of chemical bond was used by Chen *et al.*, who fabricated a hydrogel made of carboxymethyl chitosan and calcium pre-crosslinked oxidized gellan gum, complemented by magnetic hydroxyapatite/gelatin microspheres loaded with antibacterial drugs to be applied in bone tissue engineering.<sup>4</sup> The incorporation of this type of particles within the scaffold increased its mechanical stability and promoted a more sustained drug release without affecting cell viability. Nonetheless, the magnetic susceptibility of the obtained structures was not tested. This type of crosslinking bonds has the advantage of not requiring any toxic initiators nor UV light for crosslinking to occur,<sup>82</sup> which renders them biocompatible and eligible to be used in combination with cells. Furthermore, it has been shown to be usable in 3D (bio)printing applications with no effects on the long-term cell viability,<sup>83</sup> thus proving this type of reaction is compatible with the desired purpose.

To target volumetric muscle loss, Wang *et al.*<sup>5</sup> developed an injectable GelMA hydrogel with magnetic nanofibers obtained by electrospinning. The hydrogel precursor solution was mixed with the fibers and C2C12 cells, and the hydrogel was cured using UV light. Afterward, the fibers were aligned using an external magnetic field, with this alignment leading to increased cell adhesion and increased myotube length and number. Furthermore, when implanted into a mouse model, the magnetic construct enhanced angiogenesis in comparison with the control (mice implanted with the hydrogel without magnetic fibers) and sham (surgery was performed, but the mice were not implanted with any hydrogel) groups.

In a study targeting neural tissue engineering, Ghaderinejad *et al.* developed an alginate hydrogel containing magnetic short polycaprolactone (PCL) nanofibers (MSNFs) aiming to induce neuronal differentiation in olfactory ectomesenchymal stem cells (OE-MSCs).<sup>7</sup> The MSNFs were proven to be orientable by an external magnetic field within the magnetic hydrogel, as in the previous study, and the storage modulus of the bioink was found to be in the range of the values reported for the brain tissue (100–1000 Pa).<sup>84</sup> Additionally, the results showed that the hydrogels containing MSNFs were able to promote the OE-MSCs neuronal differentiation.

Another biomedical application of magnetic hydrogels is their use in hyperthermia anticancer therapies. This type of therapy takes advantage of an external alternating magnetic field to stimulate the magnetic nanoparticles present within the hydrogel. When this stimulus is applied, the MNPs dissipate heat through relaxation losses and hysteresis, and this heat then causes the death of the surrounding cancer cells.<sup>85</sup> Given that this heat release can cause unwanted damage to cells neighboring the tumor, it is crucial for the hydrogel to be accurately injected into the desired location. For this purpose, Qian *et al.* constructed an injectable silk fibroin hydrogel (FSH) with confined polyethylene glycol stabilized hydrophilic iron oxide nanocubes (IONCs) and evaluated its effectiveness in the targeting and ablation of tumors.<sup>9</sup> The scaffolds showed good injectability and a quick response to an external magnetic field. Furthermore, its self-healing behavior was tested and proven, which is crucial for the recovery of the gel state following injection. Finally, after implantation in mouse and rabbit models, its hyperthermic effects were observed.

Extensive research has been made regarding the injectability of hydrogels and its applicability in several domains of research.<sup>86,87</sup> Besides its applications in the local delivery of hydrogels in a highly precise manner and through non-invasive methods,<sup>88</sup> we reckon that the results of these works can show whether a bioink formulation possesses the right mechanical and rheological features to manufacture a solid 3D structure via a 3D (bio) printing process. This demonstrates the current potential of injectable magnetic hydrogels and its potential to be applied in 3D (bio)printing approaches.

## 6. Conclusion and future perspectives

With a broad spectrum of applications, magnetic hydrogels are used not only in several branches of tissue engineering, for example, neural, muscle, cartilage, and bone tissue regeneration, but also as antibacterial

agents and in tumor ablation strategies. Moreover, it is expected that magnetic hydrogels will be employed as smart advanced biosystems in emerging fields such as soft robotics. Furthermore, 3D (bio)printing of these stimuli-responsive materials will allow for the scalable and reproducible fabrication of constructs with complex structures able to mimic the properties of the native tissues and to be externally stimulated to foster regenerative processes. Additionally, the incorporation of magnetic particles into hydrogels also allows a better modulation of the hydrogels' features, since an external magnetic field can control the positioning of the MNPs within the scaffold, conferring different properties to different locations of the scaffold, which might contribute to the recapitulation of highly heterogeneous tissues.

However, there are still some issues that need to be further optimized for their effective implementation. Regarding the use of 3D-(bio)printed magnetic hydrogels for tissue engineering applications, there have been conflicting reports concerning the effect of the introduction of MNPs within the hydrogel matrix. Some studies have reported the improvement of mechanical properties, which translate to increased stiffness and higher Young's modulus, due to the interaction of these particles with the polymer chains. However, other works claimed that the introduction of MNPs disturbs the bonds between chains within the hydrogel, thus decreasing their mechanical performance. Therefore, further research is needed to define, more specifically, how these particles interact with their surrounding matrix, in order to accurately tune the scaffolds features.

MNPs—more specifically magnetite and maghemite—have been shown to be cytocompatible in several *in vitro* and *in vivo* animal studies. Nevertheless, given that the human body consists of several complex systems whose interaction is not accurately represented by these models, it is crucial that magnetic hydrogels can be tested in more advanced *in vitro* humanized models and in clinical trials in order to move toward the final goal of their implementation into clinical practice.

Finally, 3D (bio)printing of cell-laden bioinks has not been very extensively explored. The incorporation of cells in the bioink allows for a more uniform dispersion of cells within the hydrogel while still allowing the precise definition of its shape and structure. Nonetheless, these magnetic bioinks must have characteristics that are compatible with cell viability—such as a shear-thinning behavior.

Overall, we envision that magnetically-responsive systems will have a great impact on tissue and organ engineering due to their unique characteristics that allow

the remote manipulation of cell-laden hydrogels and the flexibility to fashion them in various shapes, which are important advantages toward the *in vitro* fabrication of a full organ.

However, more research studies are warranted, especially regarding full organ engineering since it is not yet possible to print a fully functional thick vascularized tissue that could be used as replacement in a clinical setting.

## Acknowledgments

“la Caixa” Foundation is acknowledged for the Postdoctoral Junior Leader Fellowship granted to Paola Sanjuan-Alberte.

## Funding

The authors acknowledge funding from FCT—Portuguese Foundation for Science and Technology (FCT/MCTES), with dedicated funding from the projects InSilico4OCReg (PTDC/EME-SIS/0838/2021), OptiBioScaffold (PTDC/EME-SIS/4446/2020) and eOnco (2022.07252.PTDC) and also through institutional funds to iBB (UIDB/04565/2020 and UIDP/04565/2020) and Associate Laboratory i4HB (LA/P/0140/2020). This project also received financial support from “la Caixa” Foundation (ID 100010434) LCF/BQ/PI22/11910025.

## Conflict of interest

The authors declare no conflicts of interest.

## Author contributions

*Conceptualization:* João C. Silva, Paola Sanjuan-Alberte

*Writing – original draft:* Duarte Almeida

*Writing – review & editing:* João C. Silva, Paola Sanjuan-Alberte, Frederico Castelo Ferreira

## Ethics approval and consent to participate

Not applicable.

## Consent for publication

Not applicable.

## Availability of data

Not applicable.

## References

- Cao H, Duan L, Zhang Y, Cao J, Zhang K. Current hydrogel advances in physicochemical and biological response-driven biomedical application diversity. *Signal Transduct Target Ther.* 2021;6(1): 426. doi: 10.1038/s41392-021-00830-x
- Wang W, Narain R, Zeng H. Hydrogels, in *Polymer Science and Nanotechnology.* 2020;Elsevier, 203–244.
- Choi Y, Kim C, Kim HS, Moon C, Lee KY. 3D Printing of dynamic tissue scaffold by combining self-healing hydrogel and self-healing ferrogel. *Colloids Surf B Biointerfaces.* 2021;208: 112108. doi: 10.1016/j.colsurfb.2021.112108
- Chen M, Tan H, Xu W, et al. A self-healing, magnetic and injectable biopolymer hydrogel generated by dual cross-linking for drug delivery and bone repair. *Acta Biomater.* 2022;153: 159–177. doi: 10.1016/j.actbio.2022.09.036
- Wang L, Li T, Wang Z, et al. Injectable remote magnetic nanofiber/hydrogel multiscale scaffold for functional anisotropic skeletal muscle regeneration. *Biomaterials.* 2022;285: 121537. doi: 10.1016/j.biomaterials.2022.121537
- Tognato R, Armiento AR, Bonfrate V, et al. A stimuli-responsive nanocomposite for 3D anisotropic cell-guidance and magnetic soft robotics. *Adv Funct Mater.* 2019;29(9): 1804647. doi: 10.1002/adfm.201804647
- Ghaderinejad P, Najmoddin N, Bagher Z, et al. An injectable anisotropic alginate hydrogel containing oriented fibers for nerve tissue engineering. *Chem Eng J.* 2021;420: 130465. doi: 10.1016/j.cej.2021.130465
- Li Y, Huang L, Tai G, et al. Graphene oxide-loaded magnetic nanoparticles within 3D hydrogel form high-performance scaffolds for bone regeneration and tumour treatment. *Compos Part Appl Sci Manuf.* 2022;152: 106672. doi: 10.1016/j.compositesa.2021.106672
- Qian K-Y, Song Y, Yan X, et al. Injectable ferrimagnetic silk fibroin hydrogel for magnetic hyperthermia ablation of deep tumor. *Biomaterials.* 2020;259: 120299. doi: 10.1016/j.biomaterials.2020.120299
- Gang F, Jiang L, Xiao Y, Zhang J, Sun X. Multi-functional magnetic hydrogel: Design strategies and applications. *Nano Sel.* 2021;2(12): 2291–2307. doi: 10.1002/nano.202100139
- Manjua AC, Cabral JMS, Portugal CAM. Magnetic field dynamic strategies for the improved control of the angiogenic effect of mesenchymal stromal cells. *Polymers.* 2021;13(11): 1883. doi: 10.3390/polym13111883
- Ishii M, Shibata R, Numaguchi Y, et al. Enhanced angiogenesis by transplantation of mesenchymal stem cell sheet created by a novel magnetic tissue engineering method. *Arterioscler Thromb Vasc Biol.* 2011;31(10): 2210–2215. doi: 10.1161/ATVBAHA.111.231100
- Gerdesmeyer L, Zielhardt P, Klüter T, et al. Stimulation of human bone marrow mesenchymal stem cells by electromagnetic transduction therapy - EMTT. *Electromagn Biol Med.* 2022;41(3): 304–314. doi: 10.1080/15368378.2022.2079672

14. Betsch M, Cristian C, Lin Y-Y, et al. Incorporating 4D into bioprinting: Real-time magnetically directed collagen fiber alignment for generating complex multilayered tissues. *Adv Healthc Mater.* 2018;7(21): 1800894. doi: 10.1002/adhm.201800894
15. Zhao Q, Xie P, Li X, Wang Y. Magnetic mesoporous silica nanoparticles mediated redox and pH dual-responsive target drug delivery for combined magnetothermal therapy and chemotherapy. *Colloids Surf Physicochem Eng Asp.* 2022;648: 129359. doi: 10.1016/j.colsurfa.2022.129359
16. Morfin-Gutierrez A, Sánchez-Orozco JL, García-Cerda LA, Puente-Urbina B. Preparation and characterization of nanocomposites based on poly(N-vinylcaprolactam) and magnetic nanoparticles for using as drug delivery system. *J Drug Deliv Sci Technol.* 2020;60: 102028. doi: 10.1016/j.jddst.2020.102028
17. Huang J, Shu Q, Wang L, Wu H, Wang AY, Mao H. Layer-by-layer assembled milk protein coated magnetic nanoparticle enabled oral drug delivery with high stability in stomach and enzyme-responsive release in small intestine. *Biomaterials.* 2015;39: 105–113. doi: 10.1016/j.biomaterials.2014.10.059
18. Soleymani M, Velashjerdi M, Shaterabadi Z, Barati A. One-pot preparation of hyaluronic acid-coated iron oxide nanoparticles for magnetic hyperthermia therapy and targeting CD44-overexpressing cancer cells. *Carbohydr Polym.* 2020;237: 116130. doi: 10.1016/j.carbpol.2020.116130
19. Zuvin M, Koçak M, Ünal Ö, et al. Nanoparticle based induction heating at low magnitudes of magnetic field strengths for breast cancer therapy. *J Magn Magn Mater.* 2019;483: 169–177. doi: 10.1016/j.jmmm.2019.03.117
20. Ali A, Shah T, Ullah R, et al. Review on recent progress in magnetic nanoparticles: Synthesis, characterization, and diverse applications. *Front Chem.* 2021;9: 629054. doi: 10.3389/fchem.2021.629054
21. Cardoso VF, Francesco A, Ribeiro C, Bañobre-López M, Martins P, Lanceros-Mendez S. Advances in magnetic nanoparticles for biomedical applications. *Adv Healthc Mater.* 2018;7(5): 1700845. doi: 10.1002/adhm.201700845
22. Podstawczyk D, Nizioł M, Szymczyk P, Wiśniewski P, Guiseppi-Elie A. 3D printed stimuli-responsive magnetic nanoparticle embedded alginate-methylcellulose hydrogel actuators. *Addit Manuf.* 2020;34: 101275. doi: 10.1016/j.addma.2020.101275
23. Simińska-Stanny J, Nizioł M, Szymczyk-Ziółkowska P, et al. 4D printing of patterned multimaterial magnetic hydrogel actuators. *Addit Manuf.* 2022;49: 102506. doi: 10.1016/j.addma.2021.102506
24. Chandekar KV, Shkir Mohd, Alshahrani T, et al. One-spot fabrication and in-vivo toxicity evaluation of core-shell magnetic nanoparticles. *Mater Sci Eng C.* 2021;122: 111898. doi: 10.1016/j.msec.2021.111898
25. Farzaneh S, Hosseinzadeh S, Samanipour R, Hatamie S. Fabrication and characterization of cobalt ferrite magnetic hydrogel combined with static magnetic field as a potential bio-composite for bone tissue engineering. *J Drug Deliv Sci Technol.* 2021;64: 102525. doi: 10.1016/j.jddst.2021.102525
26. Manjua AC, Cabral JMS, Portugal CAM, Ferreira FC. Magnetic stimulation of the angiogenic potential of mesenchymal stromal cells in vascular tissue engineering. *Sci Technol Adv Mater.* 2021;22(1): 461–480. doi: 10.1080/14686996.2021.1927834
27. Zhang T, Li G, Miao Y, et al. Magnetothermal regulation of in vivo protein corona formation on magnetic nanoparticles for improved cancer nanotherapy. *Biomaterials.* 2021;276: 121021. doi: 10.1016/j.biomaterials.2021.121021
28. Bonhome-Espinosa AB, Campos F, Durand-Herrera D, et al. In vitro characterization of a novel magnetic fibrin-agarose hydrogel for cartilage tissue engineering. *J Mech Behav Biomed Mater.* 2020;104: 103619. doi: 10.1016/j.jmbbm.2020.103619
29. Schneider-Futschik EK, Reyes-Ortega F. Advantages and disadvantages of using magnetic nanoparticles for the treatment of complicated ocular disorders. *Pharmaceutics.* 2021;13(8): 1157. doi: 10.3390/pharmaceutics13081157
30. Murray CB, Kagan CR, Bawendi MG. Synthesis and characterization of monodisperse nanocrystals and close-packed nanocrystal assemblies. *Annu Rev Mater Sci.* 2000;30(1): 545–610. doi: 10.1146/annurev.matsci.30.1.545
31. Anik MI, Hossain MK, Hossain I, Mahfuz AMUB, Rahman MT, Ahmed I. Recent progress of magnetic nanoparticles in biomedical applications: A review. *Nano Sel.* 2021;2(6): 1146–1186. doi: 10.1002/nano.202000162
32. Jolivet J-P, Chanéac C, Tronc E. Iron oxide chemistry. From molecular clusters to extended solid networks. *Chem Commun.* 2004;(5): 477–483. doi: 10.1039/B304532N
33. Bohara RA, Thorat ND, Pawar SH. Role of functionalization: Strategies to explore potential nano-bio applications of magnetic nanoparticles. *RSC Adv.* 2016;6(50): 43989–44012. doi: 10.1039/C6RA02129H
34. Tang J, Qiao Y, Chu Y, et al. Magnetic double-network hydrogels for tissue hyperthermia and drug release. *J Mater Chem B.* 2019;7: 1311–1321. doi: 10.1039/c8tb03301c

35. Miyazaki T, Iwanaga A, Shirosaki Y, Kawashita M. In situ synthesis of magnetic iron oxide nanoparticles in chitosan hydrogels as a reaction field: Effect of cross-linking density. *Colloids Surf B Biointerfaces*. 2019;179: 334–339. doi: 10.1016/j.colsurfb.2019.04.004
36. Gul S, Khan SB, Rehman IU, Khan MA, Khan MI. A comprehensive review of magnetic nanomaterials modern day theranostics. *Front Mater*. 2019;6: 179. doi: 10.3389/fmats.2019.00179
37. Labusca L, Herea D-D, Emanuela Minuti A, et al. Magnetic nanoparticles and magnetic field exposure enhances chondrogenesis of human adipose derived mesenchymal stem cells but not of Wharton jelly mesenchymal stem cells. *Front Bioeng Biotechnol*. 2021;9: 737132. doi: 10.3389/fbioe.2021.737132
38. Lu A-H, Salabas EL, Schüth F. Magnetic nanoparticles: Synthesis, protection, functionalization, and application. *Angew Chem Int Ed*. 2007;46(8): 1222–1244. doi: 10.1002/anie.200602866
39. Frey NA, Peng S, Cheng K, Sun S. Magnetic nanoparticles: Synthesis, functionalization, and applications in bioimaging and magnetic energy storage. *Chem Soc Rev*. 2009;38(9): 2532. doi: 10.1039/b815548h
40. Ansari S, Ficiarà E, Ruffinatti F, et al. Magnetic iron oxide nanoparticles: Synthesis, characterization and functionalization for biomedical applications in the central nervous system. *Materials*. 2019;12(3): 465. doi: 10.3390/ma12030465
41. Ali F, Khan I, Chen J, Akhtar K, Bakhsh EM, Khan SB. Emerging fabrication strategies of hydrogels and its applications. *Gels*. 2022;8(4): 205. doi: 10.3390/gels8040205
42. Mañas-Torres MC, Gila-Vilchez C, Durán JDG, Modesto T. LopezLopez, Cienfuegos LÁ de. Biomedical applications, in *Biomedical Applications of Magnetic Hydrogels*. 2021;253-271 doi: 10.1016/B978-0-12-823688-8.00020-X
43. Materón EM, Miyazaki CM, Carr O, et al. Magnetic nanoparticles in biomedical applications: A review. *Appl Surf Sci Adv*. 2021;6: 100163. doi: 10.1016/j.apsadv.2021.100163
44. Gutiérrez L, De La Cueva L, Moros M, et al. Aggregation effects on the magnetic properties of iron oxide colloids. *Nanotechnology*. 2019;30(11): 112001. doi: 10.1088/1361-6528/aafbff
45. Nardecchia S, Jiménez A, Morillas JR, et al. Synthesis and rheological properties of 3D structured self-healing magnetic hydrogels. *Polymer*. 2021;218: 123489. doi: 10.1016/j.polymer.2021.123489
46. Hu X, Nian G, Liang X, et al. Adhesive tough magnetic hydrogels with high Fe<sub>3</sub>O<sub>4</sub> content. *ACS Appl Mater Interfaces*. 2019;11(10): 10292–10300. doi: 10.1021/acsami.8b20937
47. Liu Z, Liu J, Cui X, Wang X, Zhang L, Tang P. Recent advances on magnetic sensitive hydrogels in tissue engineering. *Front Chem*. 2020;8: 124. doi: 10.3389/fchem.2020.00124
48. Koons GL, Mikos AG. Progress in three-dimensional printing with growth factors. *J Controlled Release*. 2019;295: 50–59. doi: 10.1016/j.jconrel.2018.12.035
49. Murphy SV, Atala A. 3D bioprinting of tissues and organs. *Nat Biotechnol*. 2014;32(8): 773–785. doi: 10.1038/nbt.2958
50. Beg S, Almalki WH, Malik A, et al. 3D printing for drug delivery and biomedical applications. *Drug Discov Today*. 2020;25(9): 1668–1681. doi: 10.1016/j.drudis.2020.07.007
51. Yi H-G, Lee H, Cho D-W. 3D printing of organs-on-chips. *Bioengineering*. 2017;4(4): 10. doi: 10.3390/bioengineering4010010
52. Duffy GL, Liang H, Williams RL, Wellings DA, Black K. 3D reactive inkjet printing of poly-ε-lysine/gellan gum hydrogels for potential corneal constructs. *Mater Sci Eng C*. 2021;131: 112476. doi: 10.1016/j.msec.2021.112476
53. Sorkio A, Koch L, Koivusalo L, et al. Human stem cell based corneal tissue mimicking structures using laser-assisted 3D bioprinting and functional bioinks. *Biomaterials*. 2018;171: 57–71. doi: 10.1016/j.biomaterials.2018.04.034
54. Tortorella S, Greco P, Valle F, et al. Laser assisted bioprinting of laminin on biodegradable PLGA substrates: Effect on neural stem cell adhesion and differentiation. *Bioprinting*. 2022;26: e00194. doi: 10.1016/j.bprint.2022.e00194
55. Gungor-Ozkerim PS, Inci I, Zhang YS, et al. Bioinks for 3D bioprinting: An overview. *Biomater Sci*. 2018;6(5): 915–946. doi: 10.1039/C7BM00765E
56. Gusmão A, Marques DMC, Torres-Garcia R, Ferreira FC, Alberte P, Leite M. Designing and prototyping a 3D printer for multi-extrusion of thermo- and photocurable hydrogels: Enabling affordable and wider access to bioprinting. *engrxiv*. 2023. doi: 10.31224/2916
57. Hölzl K, Lin S, Tytgat L, Vlierberghe SV, Gu L, Ovsianikov A. Bioink properties before, during and after 3D bioprinting. *Biofabrication*. 2016;8(3): 032002. doi: 10.1088/1758-5090/8/3/032002
58. Theus AS, Ning L, Kabboul G, et al. 3D bioprinting of nanoparticle-laden hydrogel scaffolds with enhanced antibacterial and imaging properties. *iScience*. 2022;25(9): 104947. doi: 10.1016/j.isci.2022.104947

59. Bartolo P, Malshe A, Ferraris E, Bahattin K. 3D bioprinting: Materials, processes, and applications. *CIRP Ann.* 2022;71(2): 577–597.  
doi: 10.1016/j.cirp.2022.06.001
60. Babaniamansour P, Salimi M, Dorkoosh F, Mohammadi M. Magnetic hydrogel for cartilage tissue regeneration as well as a review on advantages and disadvantages of different cartilage repair strategies. *BioMed Res Int.* 2022;2022: 1–12.  
doi: 10.1155/2022/7230354
61. Han X, Chang S, Zhang M, Bian X, Li C, Li D. Advances of hydrogel-based bioprinting for cartilage tissue engineering. *Front Bioeng Biotechnol.* 2021;9: 746564.  
doi: 10.3389/fbioe.2021.746564
62. Rider P, Kačarević ŽP, Alkildani S, Retnasingh S, Barbeck M. Bioprinting of tissue engineering scaffolds. *J Tissue Eng.* 2018;9: 204173141880209.  
doi: 10.1177/2041731418802090
63. Li X, Liu B, Pei B, et al. Inkjet bioprinting of biomaterials. *Chem Rev.* 2020;120(19): 10793–10833.  
doi: 10.1021/acs.chemrev.0c00008
64. Spangenberg J, Kilian D, Czichy C, et al. Bioprinting of magnetically deformable scaffolds. *ACS Biomater Sci Eng.* 2021;7(2): 648–662.  
doi: 10.1021/acsbmaterials.0c01371
65. Kabir W, Di Bella C, Choong PFM, O'Connell CD. Assessment of native human articular cartilage: A biomechanical protocol. *Cartilage.* 2021;13(2\_suppl): 427S–437S.  
doi: 10.1177/1947603520973240
66. Chang S, Wang S, Liu Z, Wang X. Advances of stimulus-responsive hydrogels for bone defects repair in tissue engineering. *Gels.* 2022;8(6): 389.  
doi: 10.3390/gels8060389
67. Pardo A, Gómez-Florit M, Barbosa S, Taboada P, Domingues RMA, Gomes ME. Magnetic nanocomposite hydrogels for tissue engineering: Design concepts and remote actuation strategies to control cell fate. *ACS Nano.* 2021;15(1): 175–209.  
doi: 10.1021/acsnano.0c08253
68. Yazdanpanah Z, Johnston JD, Cooper DML, Chen X. 3D bioprinted scaffolds for bone tissue engineering: State-of-the-art and emerging technologies. *Front Bioeng Biotechnol.* 2022;10: 824156.  
doi: 10.3389/fbioe.2022.824156
69. Jana S, Levengood SKL, Zhang M. Anisotropic materials for skeletal-muscle-tissue engineering. *Adv Mater.* 2016;28(48): 10588–10612.  
doi: 10.1002/adma.201600240
70. Hwangbo H, Lee H, Jin E-J, et al. Bio-printing of aligned GelMa-based cell-laden structure for muscle tissue regeneration. *Bioact Mater.* 2022;8: 57–70.  
doi: 10.1016/j.bioactmat.2021.06.031
71. Ajiteru O, Choi KY, Lim TH, et al. A digital light processing 3D printed magnetic bioreactor system using silk magnetic bioink. *Biofabrication.* 2021;13(3): 034102.  
doi: 10.1088/1758-5090/abfae
72. Mertz D, Harlepp S, Goetz J, et al. Nanocomposite polymer scaffolds responding under external stimuli for drug delivery and tissue engineering applications. *Adv Ther.* 2020;3(2): 1900143.  
doi: 10.1002/adtp.201900143
73. Ostrovidov S, Salehi S, Costantini M, et al. 3D bioprinting in skeletal muscle tissue engineering. *Smal.* 2019;15(24): 1805530.  
doi: 10.1002/sml.201805530
74. Wang Z, Wang L, Li T, et al. 3D bioprinting in cardiac tissue engineering. *Theranostics.* 2021;11(16): 7948–7969.  
doi: 10.7150/thno.61621
75. Allafchian A, Hosseini SS. Antibacterial magnetic nanoparticles for therapeutics: A review. *IET Nanobiotechnol.* 2019;13(8): 786–799.  
doi: 10.1049/iet-nbt.2019.0146
76. Franco D, Calabrese G, Guglielmino SPP, Conoci S. Metal-based nanoparticles: Antibacterial mechanisms and biomedical application. *Microorganisms.* 2022;10(9): 1778.  
doi: 10.3390/microorganisms10091778
77. Xu C, Akakuru OU, Zheng J, et al. Applications of iron oxide-based magnetic nanoparticles in the diagnosis and treatment of bacterial infections. *Front Bioeng Biotechnol.* 2019;7: 141.  
doi: 10.3389/fbioe.2019.00141
78. Lee Y, Song WJ, Sun J-Y. Hydrogel soft robotics. *Mater Today Phys.* 2020;15: 100258.  
doi: 10.1016/j.mtphys.2020.100258
79. Janarthanan G, Noh I. *Overview of Injectable Hydrogels for 3D Bioprinting and Tissue Regeneration in Injectable Hydrogels for 3D Bioprinting*, ed I, The Royal Society of Chemistry. 2021;1–20.  
doi: 10.1039/9781839163975-00001
80. Devi VKA, Shyam R, Palaniappan A, Jaiswal AK, Oh T-H, Nathanael AJ. Self-healing hydrogels: Preparation, mechanism and advancement in biomedical applications. *Polymers.* 2021;13(21): 3782.  
doi: 10.3390/polym13213782
81. Raczuk E, Dmochowska B, Samaszko-Fiertek J, Madaj J. Different schiff bases — structure, importance and classification. *Molecules.* 2022;27(3): 787.  
doi: 10.3390/molecules27030787
82. Janarthanan G, Tran HN, Cha E, Lee C, Das D, Noh I. 3D printable and injectable lactoferrin-loaded carboxymethyl cellulose-glycol chitosan hydrogels for tissue engineering applications. *Mater Sci Eng C.* 2020;113: 111008.  
doi: 10.1016/j.msec.2020.111008

83. Puertas-Bartolomé M, Włodarczyk-Biegun MK, del Campo A, Vázquez-Lasa B, Román JS. 3D printing of a reactive hydrogel bio-ink using a static mixing tool. *Polymers*. 2020;12(9): 1986. doi: 10.3390/polym12091986
84. Banerjee A, Arha M, Choudhary S, et al. The influence of hydrogel modulus on the proliferation and differentiation of encapsulated neural stem cells. *Biomaterials*. 2009;30(27): 4695–4699. doi: 10.1016/j.biomaterials.2009.05.050
85. Ganguly S, Margel S. 3D printed magnetic polymer composite hydrogels for hyperthermia and magnetic field driven structural manipulation. *Prog Polym Sci*. 2022;131: 101574. doi: 10.1016/j.progpolymsci.2022.101574
86. Rizzo F, Kehr NS. Recent advances in injectable hydrogels for controlled and local drug delivery. *Adv Healthc Mater*. 2021;10(1): 2001341. doi: 10.1002/adhm.202001341
87. Almawash S, Osman SK, Mustafa G, El Hamd MA. Current and future prospective of injectable hydrogels—design challenges and limitations. *Pharmaceuticals*. 2022;15(3): 371. doi: 10.3390/ph15030371
88. Gao F, Jiao C, Yu B, Cong H, Shen Y. Preparation and biomedical application of injectable hydrogels. *Mater Chem Front*. 2021;5: 4912–4936. doi: 10.1039/D1QM00489A
89. Pavón JJ, Allain JP, Verma D, et al. In situ study unravels bio-nanomechanical behavior in a magnetic bacterial nano-cellulose (MBNC) hydrogel for neuro-endovascular reconstruction. *Macromol Biosci*. 2019;19(2): 1800225. doi: 10.1002/mabi.201800225
90. Flood-Garibay JA, Méndez-Rojas MA. Synthesis and characterization of magnetic wrinkled mesoporous silica nanocomposites containing Fe<sub>3</sub>O<sub>4</sub> or CoFe<sub>2</sub>O<sub>4</sub> nanoparticles for potential biomedical applications. *Colloids Surf Physicochem Eng Asp*. 2021;615: 126236. doi: 10.1016/j.colsurfa.2021.126236
91. Fernández I, Carinelli S, González-Mora JL, Villalonga R, Lecuona M, Salazar P. Electrochemical bioassay based on l-lysine-modified magnetic nanoparticles for Escherichia coli detection: Descriptive results and comparison with other commercial magnetic beads. *Food Control*. 2023;145: 109492. doi: 10.1016/j.foodcont.2022.109492
92. Sartori K, Choueikani F, Gloter A, Begin-Colin S, Taverna D, Pichon BP. Room temperature blocked magnetic nanoparticles based on ferrite promoted by a three-step thermal decomposition process. *J Am Chem Soc*. 2019;141(25): 9783–9787. doi: 10.1021/jacs.9b03965
93. Tomar D, Jeevanandam P. Synthesis of cobalt ferrite nanoparticles with different morphologies via thermal decomposition approach and studies on their magnetic properties. *J Alloys Compd*. 2020;843: 155815. doi: 10.1016/j.jallcom.2020.155815
94. Kim D, Lee N, Park M, Kim BH, An K, Hyeon T. Synthesis of uniform ferrimagnetic magnetite nanocubes. *J Am Chem Soc*. 2009;131(2): 454–455. doi: 10.1021/ja8086906
95. Shibaev A, Smirnova M, Kessel D, Bedin SA, Razumovskaya IV, Philippova OE. Remotely self-healable, shapeable and pH-sensitive dual cross-linked polysaccharide hydrogels with fast response to magnetic field. *Nanomaterials*. 2021;11(5): 1271. doi: 10.3390/nano11051271